

# Probing the pole origin of $X(3872)$ with the coupled-channel dynamics

Jun-Zhang Wang <sup>1,\*</sup> Zi-Yang Lin <sup>1,†</sup> Yan-Ke Chen <sup>1,‡</sup> Lu Meng <sup>2,§</sup> and Shi-Lin Zhu <sup>1,¶</sup>

<sup>1</sup>*School of Physics and Center of High Energy Physics, Peking University, Beijing 100871, China*

<sup>2</sup>*Institut für Theoretische Physik II, Ruhr-Universität Bochum, D-44780 Bochum, Germany*

(Dated: April 26, 2024)

The  $X(3872)$ , as the first and the most crucial member in the exotic charmoniumlike  $XYZ$  family, has been studied for a long time. However, its dynamical origin, whether stemming from a  $D\bar{D}^*$  hadronic molecule or the first excited  $P$ -wave charmonium  $\chi_{c1}(2P)$ , remains controversial. In this Letter, we demonstrate that the  $X(3872)$  definitely does not result from the mass shift of the higher bare  $\chi_{c1}(2P)$  resonance pole in the coupled-channel dynamics involving a short-distance  $c\bar{c}$  core and the long-distance  $D\bar{D}^*$  channels. Instead, it originates from either the  $D\bar{D}^*$  molecular pole or the shadow pole associated with the  $P$ -wave charmonium, which depends on the concrete coupling mode between the  $c\bar{c}$  and  $D\bar{D}^*$ . In order to further exploit the nature of  $X(3872)$ , we carefully investigate potential mechanisms that contribute to its pole width, which suggests that the coupled-channel dynamics plays a critical role in causing a noticeable discrepancy between the pole widths of  $X(3872)$  and  $T_{cc}^+$ . Interestingly, we bridge the quantitative connection among the dynamics origin of  $X(3872)$ , its pole width and the properties of the predicted new resonance. The precise measurement of the pole width of  $X(3872)$  and the search for the new charmoniumlike resonance become highly significant and can be anticipated in future LHCb, BESIII and Belle II experiments.

*Introduction.*— During the past two decades, one of the most important topics in the physics of the strong interaction is to understand a large number of charmoniumlike  $XYZ$  resonances observed by high energy experiments including BaBar, Belle, BESIII and LHCb, and so on (see Refs. [1–6] for relevant progresses). As a superstar among them, the nature of  $X(3872)$  is the most mysterious, which is mainly manifested in that its mass exactly coincides to the threshold of  $D^0\bar{D}^{*0}/D^{*0}\bar{D}^0$  and its decay pattern is strongly coupled with  $D^0\bar{D}^0\pi^0$  [7, 8]. These behaviors imply the central role of  $D\bar{D}^*$  ( $D\bar{D}^*$  refers to  $D\bar{D}^*/\bar{D}D^*$  and similarly hereinafter) in the generation of  $X(3872)$ . As a result, the hadronic molecular interpretation of  $X(3872)$  was naturally proposed [9–14]. Intriguingly, the LHCb Collaboration recently discovered the doubly charmed tetraquark  $T_{cc}^+$  in the prompt production of the  $p\bar{p}$  collision [15, 16], which has been widely acknowledged as an ideal candidate for the shallow  $DD^*$  bound state [17–42].

Compared with the doubly charmed tetraquark  $T_{cc}^+$ , a more complicated aspect of  $X(3872)$  is that its  $D\bar{D}^*$  component inevitably interacts with the conventional  $P$ -wave charmonium states with the same quantum number  $J^{PC} = 1^{++}$  [43, 44], especially the nearby  $\chi_{c1}(2P)$  state (hereinafter denoted as  $\chi'_{c1}$ ). Therefore, it can be expected that the realistic wave function of  $X(3872)$  should behave as a compact charmonium core in the short-distance region and a  $D\bar{D}^*$  structure in the long-distance region [45–48]. In this coupled-channel framework, a prevalent opinion suggests that the  $X(3872)$  arises from the mass shift of the higher  $\chi'_{c1}$  state due to the unquenched  $D\bar{D}^*$  loop correction to the self-energy of the  $P$ -wave charmonium [49–55]. Thus, whether the  $X(3872)$  is a hadronic molecule or an excited charmonium remains controversial. Regarding this long-standing view, in this Letter, we demonstrate that the  $X(3872)$  definitely does not originate from the bare  $\chi'_{c1}$  resonance pole in the coupled-channel dynamics involving the  $c\bar{c}$  core and the  $D\bar{D}^*$  channels. The

$X(3872)$  stems from either the  $D\bar{D}^*$  pole in the so-called weak-coupling mode or the shadow pole associated with  $\chi'_{c1}$  in the strong-coupling mode.

To further decipher the nature of  $X(3872)$ , we systematically investigate the pole width of  $X(3872)$ . We establish the  $D\bar{D}^*$  interaction with the chiral effective field theory (ChEFT), and the transition amplitude between the  $P$ -wave charmonium and  $D\bar{D}^*$  with the quark-pair-creation (QPC) model. We explore three kinds of potential mechanisms contributing to the pole width, namely the  $D\bar{D}^*\pi$  three-body cut from the one-pion exchange (OPE) in the  $D\bar{D}^*$  scattering, the dynamical width of  $\bar{D}^*$  and the non-open-charm decays of the bare  $\chi'_{c1}$  state. We find that the coupled-channel dynamics plays a crucial role in generating a significantly larger pole width of  $X(3872)$  compared with that of  $T_{cc}^+$ . Furthermore, we establish a quantitative connection among the dynamical origin of  $X(3872)$ , its pole width and the properties of the predicted new resonance, which underscores the importance of precise measurements of the pole width of  $X(3872)$  in future high-energy experiments. These findings should constitute an important step towards thoroughly unraveling the mystery of  $X(3872)$  and constructing the  $P$ -wave charmonium family.

*Pole evolution of  $X(3872)$  in the coupled-channel dynamics.*— We adopt a complete coupled-channel framework to study the properties of  $X(3872)$ , in which the  $D\bar{D}^*$  scattering dynamics is also included. The hadronic fock state can be written as

$$|\Phi\rangle = c_0|\Phi_0\rangle + \sum_i \int \frac{d^3\mathbf{q}}{(2\pi)^3} \phi_i(\mathbf{q})|\Phi_i\rangle_{\mathbf{q}}, \quad (1)$$

where  $|\Phi_0\rangle$  and  $|\Phi_i\rangle_{\mathbf{q}}$  correspond to the bare fock state and the  $i$ -channel hadron-hadron continuum state associated with the relative momentum  $\mathbf{q}$ , respectively. Then the coupled-channel

Schrödinger equation can be written as

$$\begin{pmatrix} \mathcal{H}_0 & \mathcal{H}_{01} & \mathcal{H}_{02} & \dots \\ \mathcal{H}_{10} & \mathcal{H}_1 & \mathcal{H}_{12} & \dots \\ \mathcal{H}_{20} & \mathcal{H}_{21} & \mathcal{H}_2 & \dots \\ \vdots & \vdots & \vdots & \ddots \end{pmatrix} \begin{pmatrix} c_0 |\Phi_0\rangle \\ |\Phi_1\rangle \\ |\Phi_2\rangle \\ \vdots \end{pmatrix} = E \begin{pmatrix} c_0 |\Phi_0\rangle \\ |\Phi_1\rangle \\ |\Phi_2\rangle \\ \vdots \end{pmatrix} \quad (2)$$

with

$$|\Phi_i\rangle = \int \frac{d^3\mathbf{q}}{(2\pi)^3} \phi_i(\mathbf{q}) |\Phi_i\rangle_{\mathbf{q}}, \quad (i = 1, 2, \dots). \quad (3)$$

After expanding the above matrix equation and applying the relation  $\langle \Phi_0 | \mathcal{H}_0 | \Phi_0 \rangle = M_0$ ,  $\langle \Phi_j |_{\mathbf{q}} \mathcal{H}_{j0} | \Phi_0 \rangle = \mathcal{V}_{0j}(\mathbf{q})$  and  $\langle \Phi_j |_{\mathbf{q}'} \mathcal{H}_{ji} | \Phi_i \rangle_{\mathbf{q}} = \delta_{ij} E_k + V_{ij}(\mathbf{q}, \mathbf{q}')$ , one can obtain

$$\sum_i \int \phi_i(\mathbf{q}) \mathcal{V}_{i0}(\mathbf{q}) \frac{d^3\mathbf{q}}{(2\pi)^3} = (E - M_0) c_0, \quad (4)$$

$$\begin{aligned} c_0 \mathcal{V}_{0j}(\mathbf{q}) + \sum_i \int (\delta_{ij} E_k + V_{ij}(\mathbf{q}, \mathbf{q}')) \phi_i(\mathbf{q}') \frac{d^3\mathbf{q}'}{(2\pi)^3} \\ = E \phi_j(\mathbf{q}) \quad (j = 1, 2, 3, \dots), \end{aligned} \quad (5)$$

respectively, where  $M_0$  is the bare mass of  $|\Phi_0\rangle$ , the  $\mathcal{V}_{0j}$  corresponds to the transition amplitude between the bare state and the  $j$ -th channel, and the  $E_k$  and  $V_{ij}$  stand for the kinetic term  $\mathbf{q}^2/(2\mu)$  and the potential of the corresponding hadron-hadron scattering, respectively. Combining Eqs. (4) and (5), we have

$$\begin{aligned} \sum_i (\delta_{ij} E_k + \int (V_{ij}(\mathbf{q}, \mathbf{q}') + \mathcal{V}_{ij}(\mathbf{q}, \mathbf{q}')) \phi_i(\mathbf{q}') \frac{d^3\mathbf{q}'}{(2\pi)^3}) \\ = E \phi_j(\mathbf{q}) \quad (j = 1, 2, 3, \dots), \end{aligned} \quad (6)$$

where  $\mathcal{V}_{ij}(\mathbf{q}, \mathbf{q}') = \frac{\mathcal{V}_{i0}(\mathbf{q}') \mathcal{V}_{0j}(\mathbf{q})}{E - M_0 + i\epsilon}$ . Equation (6) is a standard coupled-channel Schrödinger equation in momentum space. The coupled-channel problem between the bare state and the hadronic continuum is converted to a hadron-hadron scattering problem including an extra  $s$ -channel effective potential  $\mathcal{V}_{ij}(\mathbf{q}, \mathbf{q}')$ .

We consider a two-channel calculation involving the  $[D^0 \bar{D}^{*0}]$  and  $[D^+ \bar{D}^{*-}]$ , where the square brackets are the shorthands of the  $C = +$  states such as  $[D^0 \bar{D}^{*0}] = \frac{1}{\sqrt{2}}(D^0 \bar{D}^{*0} - \bar{D}^0 D^{*0})$ . Because the mass of  $X(3872)$  lies close to the threshold of  $D^0 \bar{D}^{*0}$ , the  $D\bar{D}^* \rightarrow D\bar{D}^*$  scattering should be governed by the leading-order contact and OPE interactions in the effective field theory [28]. The total effective potential can be written as

$$V_{\text{Total}}(\mathbf{q}, \mathbf{q}') = \begin{pmatrix} C_t - V_{\pi^0} + \mathcal{V}_{11} & C'_t - 2V_{\pi^\pm} + \mathcal{V}_{12} \\ C'_t - 2V_{\pi^\pm} + \mathcal{V}_{21} & C_t - V_{\pi^0} + \mathcal{V}_{22} \end{pmatrix}, \quad (7)$$

where  $C_t$  and  $C'_t$  are the contact terms,  $V_\pi$  is the OPE potential and  $\mathcal{V}_{11} = \mathcal{V}_{12} = \mathcal{V}_{21} = \mathcal{V}_{22}$ . Since the ChEFT only works at small momentum, we introduce a Gaussian cutoff to regularize the contact and OPE potential, i.e.,

$$\mathcal{F}(\mathbf{q}, \mathbf{q}') = \exp(-(\mathbf{q}^2 + \mathbf{q}'^2)/\Lambda^2), \quad (8)$$

where the cutoff  $\Lambda = 0.5$  GeV is usually taken for the  $DD^*$  or  $D\bar{D}^*$  system [28]. In order to explore the trajectory of the pole generated in the  $D\bar{D}^* \rightarrow D\bar{D}^*$  scattering in the coupled-channel dynamics, we first ignore the OPE contribution and adopt the momentum-dependent form of  $\mathcal{V} = \frac{g^2}{2M_0} e^{-(\mathbf{q}^2 + \mathbf{q}'^2)/\alpha^2} / (E - M_0 + i\epsilon)$ , where  $\alpha$  and  $g$  characterize the coupling range and strength between  $\chi'_{c1}$  and  $D\bar{D}^*$ , respectively. Then the effective potential in Eq. (7) becomes separable, and it would be very convenient to analytically solve the Lippmann-Schwinger equation (LSE) and search for the poles of the  $T$  matrix [56].

The general coupled-channel LSE is given by

$$T_\beta^\alpha(q, q') = V_\beta^\alpha(q, q') + \sum_\gamma \int_0^\infty \frac{dk k^2}{(2\pi)^3} \frac{V_\gamma^\alpha(q, k) T_\beta^\gamma(k, q')}{E - k^2 / (2\mu_\gamma)}, \quad (9)$$

where  $V_\beta^\alpha(q, q')$  is the partial-wave-projected potential from the  $\alpha$  channel to the  $\beta$  channel, and  $q$  and  $q'$  correspond to the initial and final momentum, respectively. The reduced mass  $\mu_\gamma$  is defined by

$$\mu_\gamma = \frac{m_1 m_2}{m_1 + m_2}. \quad (10)$$

With the above preparations, we investigate the pole origin of  $X(3872)$ . We first focus on the situation with the strict isospin symmetry, in which the two-channel calculation in Eq. (9) is reduced to a single-channel one. The pole trajectories in the momentum  $k_0$ -plane are presented in Fig. 1. Here,  $k_0$  is defined by  $k_0 = \sqrt{2\mu(E - m_D - m_{D^*})}$ .  $k_0$  with positive and negative imaginary parts correspond to the first and second Riemann sheets of the  $T$  matrix, respectively. The bare mass  $M_0 = 3.96$  GeV is adopted according to the quark model estimations [57, 58]. The subfigures 1, 2, 3 represent the cases with no contact interaction ( $C_t = 0$  GeV $^{-2}$ ), an attractive contact interaction ( $C_t = -10$  GeV $^{-2}$ ) and a repulsive contact interaction ( $C_t = 10$  GeV $^{-2}$ ), respectively. In Fig. 1(a) and (b), we show the pole trajectories of the  $D\bar{D}^*$  scattering when increasing the coupling strength  $g$  in the so-called weak coupling mode with a typical value  $\alpha = 1.0$  GeV and in the strong coupling mode with  $\alpha = 1.4$  GeV, respectively, which indicates a smaller and larger overlap range between the wave functions of the  $c\bar{c}$  core and  $D\bar{D}^*$  channel, respectively.

In Fig. 1(a-1) with the weak coupling mode, there appear three poles of the  $T$  matrix in the complex plane, although only the  $s$ -channel interaction  $\mathcal{V}$  is considered. It is easy to identify the nature of these three poles by setting  $g^2 \rightarrow 0$ . The red, blue and green poles correspond to the bare  $\chi'_{c1}$  resonance, the shadow pole associated with  $\chi'_{c1}$  resonance and a virtual state of  $D\bar{D}^*$  at the infinity, respectively. With gradually increasing  $g^2$ , the pole of  $\chi'_{c1}$  resonance moves first towards and then away from the threshold of  $D\bar{D}^*$ , while the  $D\bar{D}^*$  virtual state continuously moves towards the threshold and finally crosses the unitary branch cut of  $D\bar{D}^*$  and becomes a bound state, which corresponds to the observed

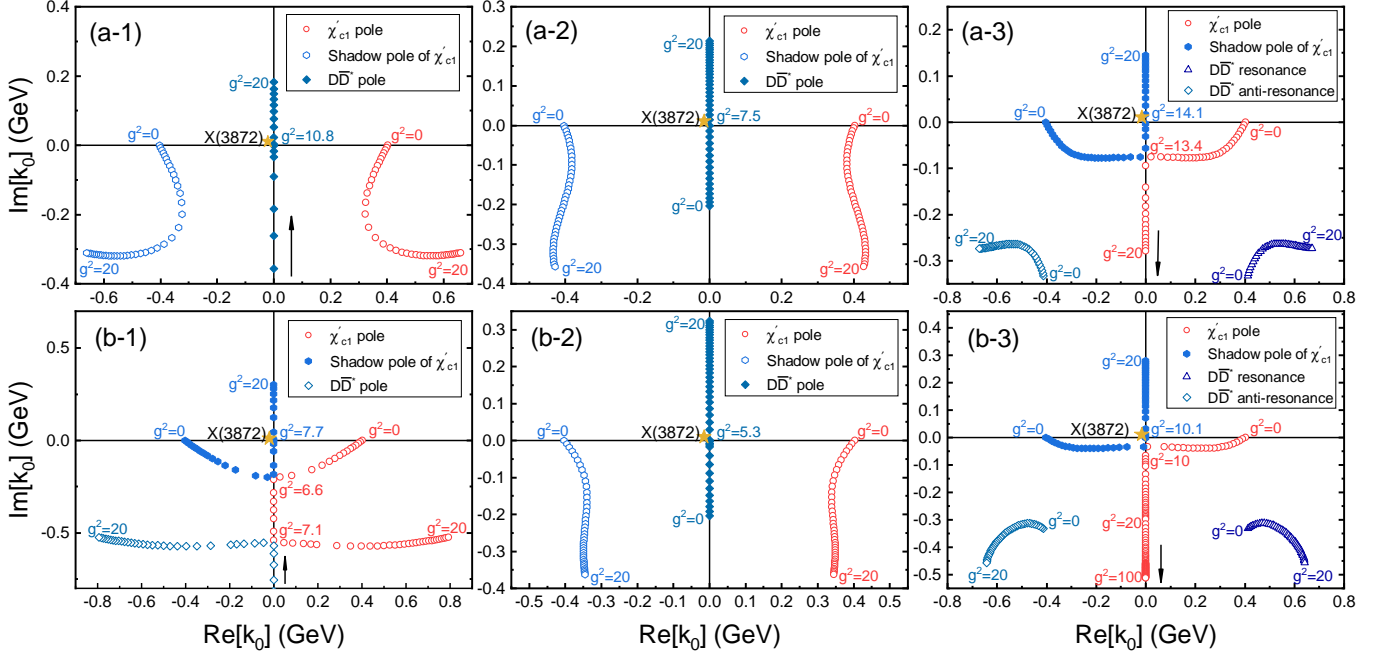


FIG. 1. The pole evolutions of the single-channel  $DD^* \rightarrow D\bar{D}^*$  scattering (no isospin violation) in the coupled-channel dynamics. Here, the complex plane refers to the momentum  $k_0$ . The subfigure (a-1), (a-2), (a-3), (b-1), (b-2) and (b-3) correspond to the  $(C_t \text{ (GeV}^{-2}), \alpha \text{ (GeV)}) = (0, 1.0), (-10, 1.0), (+10, 1.0), (0, 1.4), (-10, 1.4)$  and  $(+10, 1.4)$ , respectively.

$X(3872)$  structure. For the strong coupling mode shown in Fig. 1(b-1), the situation is completely different. When  $g^2$  increases to a critical value, the  $\chi'_{c1}$  pole and its shadow pole will meet at the same point as virtual states and then continue to move along the negative imaginary axis of the  $k_0$ -plane in opposite directions. Subsequently, the  $\chi'_{c1}$  pole will meet the  $D\bar{D}^*$  virtual state pole arising from the infinity and then they evolve into a pair of resonance and anti-resonance. In contrast, the shadow pole associated with  $\chi'_{c1}$  will enter the first Riemann sheet and be related to a  $X(3872)$  structure.

It is important to highlight that this pole separation behavior associated with the  $\chi'_{c1}$  state is directly attributed to the tiny imaginary part  $i\epsilon$  of the effective potential  $\mathcal{V} \propto (m_{th} + k_0^2/(2\mu) - M_0 + i\epsilon)^{-1}$ . Thus, such a phenomenon is still universal when including the intrinsic  $DD^*$  dynamics, as shown in Fig. 1(a-2), (a-3), (b-2) and (b-3). It can be seen that an intrinsic attractive force between  $D$  and  $\bar{D}^*$  prompts the pole evolution behaviors to favor the weak coupling mode and a repulsive force causes poles to evolve in favor of the strong coupling mode. Interestingly, due to the influence of the repulsive interaction, the  $\chi'_{c1}$  pole might continuously emerge as a virtual state by a strong enough threshold coupling. To sum up, whatever the dynamics origin of  $X(3872)$  is,  $X(3872)$  does not originate from the mass shift of the bare  $\chi'_{c1}$  resonance pole in the coupled-channel dynamics.

For  $X(3872)$ , the isospin breaking effect is significant since the mass difference between the neutral and charged channels is up to 8 MeV [59]. Thus, we further study the pole evolu-

tion of  $DD^* \rightarrow D\bar{D}^*$  in the two-channel scattering, which is presented in Fig. 2. Here, in order to make the  $T$ -matrix a single-valued function in the locally flat surface, a uniformization variable  $z$  is introduced to achieve a mapping from energy  $E$  to  $z$  [60–62], whose definition is summarized in Appendix. In the  $z/E$ -plane of Fig. 2, the orange and black solid lines stand for the unitary branch cuts related to the  $[D^0\bar{D}^{*0}]$  and  $[D^+\bar{D}^{*-}]$ , respectively. The dashed lines represent the real axis of the  $E$ -plane unoccupied by the branch cut. The four Riemann sheets  $(+, +)$ ,  $(-, +)$ ,  $(+, -)$  and  $(-, -)$  for the two-channel system correspond to the upper half  $z$ -plane outside and inside the circle, and the lower half  $z$ -plane inside and outside the circle, respectively, where  $+$  and  $-$  represent the first and the second Riemann sheets, respectively.

Since the impact of the intrinsic  $DD^*$  dynamics on the pole evolution in the two-channel case is very similar to the lesson learned from the single-channel analysis, here we only show the two-channel calculations with  $C_t = C'_t = 0 \text{ GeV}^{-2}$ . In Fig. 2(a-1) with a typical value  $\alpha = 1.0 \text{ GeV}$ , a large number of new poles appear due to the isospin symmetry violation, and it can be found that the evolution behaviors of the dressed  $\chi'_{c1}$  resonance and its shadow pole in the  $(-, -)$  sheet are very similar to those of the weak coupling mode in the single-channel case. However, the  $X(3872)$  pole no longer arises from the virtual  $DD^*$  state in the  $(-, -)$  sheet. Instead, it arises from the shadow resonance of  $\chi'_{c1}$  in the  $(-, +)$  sheet. In Fig. 2(a-2), we show the corresponding pole trajectories in the complex energy plane. It can be seen that the dressed  $\chi'_{c1}$  resonance is always higher than the  $[D^+\bar{D}^{*-}]$  threshold.

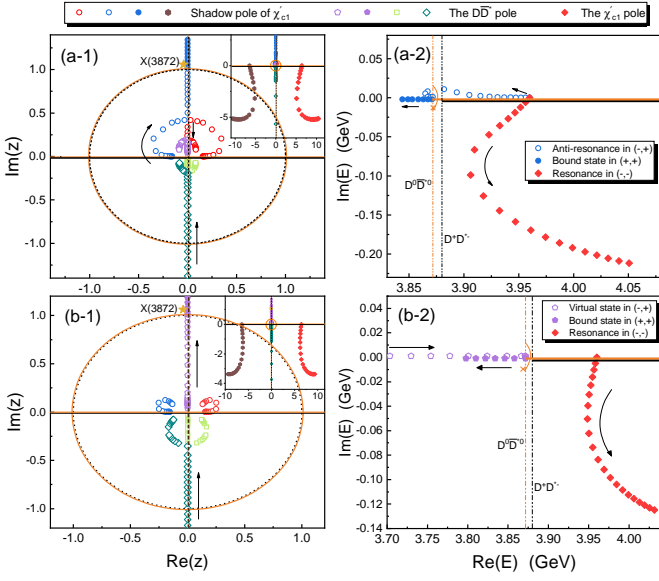


FIG. 2. The pole evolutions of the two-channel  $DD^* \rightarrow DD^*$  scattering (isospin violation) in the coupled-channel dynamics. Left and right figures are related to the uniformization  $z$ -plane and the corresponding energy  $E$ -plane. It is worth emphasizing that the solid and hollow blue (purple) points refer to the same pole.

Its shadow pole in the  $(-, +)$  sheet first moves into the energy region below the  $[D^0 \bar{D}^{*0}]$  threshold and then returns and crosses the unitary cut of  $[D^0 \bar{D}^{*0}]$  into the  $(+, +)$  sheet and becomes a bound state  $X(3872)$ . This trajectory is still maintained when employing a stronger coupling mode such as  $\alpha = 1.4$  GeV. However, when adopting a weaker coupling mode ( $\alpha = 0.8$  GeV), as presented in Fig. 2(b-1) and (b-2), the shadow pole of  $\chi'_{c1}$  in the  $(-, +)$  sheet will not be pulled to the imaginary axis of the  $z$ -plane and the  $X(3872)$  originates from a  $DD^*$  virtual state pole in the  $(-, +)$  sheet.

*The pole width of  $X(3872)$  and the relevant implications.*— Recently, the LHCb Collaboration and BESIII Collaboration extracted the pole position of  $X(3872)$  by analyzing the line shape, whose imaginary part is extracted to be  $-(130^{+320}_{-180})i$  keV [63] and  $-(190^{+206}_{-161})i$  keV [64], respectively. Although the experimental errors are large, both of the center values are obviously larger than that of  $T_{cc}^+$ , which is extracted to be  $-(48 \pm 2)i$  keV [15, 16]. The pole width of  $T_{cc}^+$  has been reproduced well in theoretical calculations and can be attributed to the dominant three-body  $DD\pi$  decay [26–29, 31]. However, the  $DD\pi$  half decay width of  $X(3872)$  from the three-body cut of the OPE potential is estimated to be only  $15 \sim 34$  keV in Refs. [28, 29]. The possible large pole width of  $X(3872)$  has not been understood well in the present theoretical studies.

Here, we conjecture that the coupled-channel dynamics plays a critical role in producing the larger pole width of  $X(3872)$ , which is completely inaccessible to the  $T_{cc}^+$ . The motivation bases on the evidence that the experimental total width of the ground state  $P$ -wave charmonium  $\chi_{c1}(1P)$ ,

whose open-charm decay channels are not opened yet, can reach  $0.88 \pm 0.05$  MeV [59]. Hence, it can be expected that the non-open-charm decay widths of the bare  $\chi'_{c1}$  state possess the same order of magnitude as that of the ground state. In order to verify this point, we employ a quark-model-independent scheme to estimate the decay behaviors of the bare  $\chi'_{c1}$  state. The main non-open-charm modes of the bare  $\chi'_{c1}$  include the radiative and light hadron decays, which is usually related to the spatial wave function of the charmonium. The radial wave function of  $\chi'_{c1}$  can be described by a simple harmonic oscillator function [65, 66], i.e.,

$$R_{nL}(r, \beta) = \beta^{\frac{3}{2}} \sqrt{\frac{2n!}{\Gamma(n+L+\frac{3}{2})}} (\beta r)^L e^{-\frac{r^2 \beta^2}{2}} L_n^{L+\frac{1}{2}}(r^2 \beta^2),$$

where  $L_n^{L+\frac{1}{2}}$  is the associated Laguerre polynomial with the orbital angular momentum  $L$  and the radial quantum number  $n$ . Under the heavy quark symmetry, it can be concluded that the  $P$ -wave charmonium triplets share the same radial wave function, so the unique unknown parameter  $\beta = 0.7 \sim 0.9$  GeV [66] can be reliably determined by the experimental total width of  $\chi'_{c2}$  and  $\chi'_{c0}$  [59]. Subsequently, the decays into light hadrons or a charmonium with a photon can be calculated. The coupling amplitude  $\mathcal{V}_{0j}(\mathbf{q})$  and  $\mathcal{V}_{i0}(\mathbf{q}')$  in Eq. (6) can also be obtained in the quark pair creation (QPC) model without extra parameter dependence. The relevant details can be found in Appendix. Now, the  $s$ -channel effective potential should be modified as

$$\mathcal{V}_{ij}(\mathbf{q}, \mathbf{q}') = \frac{\mathcal{V}_{i0}(\mathbf{q}') \mathcal{V}_{0j}(\mathbf{q})}{E - M_0 + i\epsilon} \rightarrow \frac{\mathcal{V}_{i0}(\mathbf{q}') \mathcal{V}_{0j}(\mathbf{q}) e^{-\lambda^2(\mathbf{q}^2 + \mathbf{q}'^2)}}{E - M_0 + i\frac{1}{2}(\Gamma_a + \Gamma_b)},$$

where  $\Gamma_a = 3488$  keV and  $\Gamma_b = 220$  keV correspond to the light hadron decays and radiative decays of the bare  $\chi'_{c1}$  when adopting  $\beta = 0.75$  GeV, respectively. According to suggestions from Refs. [67–69], an extra cutoff parameter  $\lambda$  is required to adjust the large momentum suppression in  $\mathcal{V}_{i0}$  from the input of the QPC amplitude. Additionally, we also simultaneously take into account the three-body  $DD\pi$  threshold effect from the OPE interaction [28] and the dynamical width of  $\bar{D}^*$  from its strong decay  $\bar{D}\pi$  and electromagnetic decay  $\bar{D}\gamma$  (see Appendix for relevant formalisms). The complete scattering amplitudes of  $DD^* \rightarrow DD^*$  involving these three potential mechanisms contributing to the pole width are presented in Fig. 3.

The inclusion of these decay dynamics makes the system Hamiltonian no longer Hermitian. For this situation, a more convenient approach to extract the pole positions of the full scattering amplitudes in Fig. 3 is the complex scaling method (CSM) based on the Schrödinger equation [70–72]. In our previous studies on  $T_{cc}^+$  in ChEFT [28], it is found that the pole width is not sensitive to the cutoff  $\Lambda$  within a large range of  $\Lambda = 0.4 - 1.0$  GeV, and then the  $\Lambda$  cutoff dependence can be safely renormalized by the contact interaction. Thus, the  $\Lambda$  is fixed to 0.5 GeV and the undetermined parameters are  $\lambda$ ,  $C_t$  and  $C'_t$ . The last two can be related to two new contact constants  $V_{ct}^{I=0}$  and  $V_{ct}^{I=1}$  (see Appendix for their definitions).

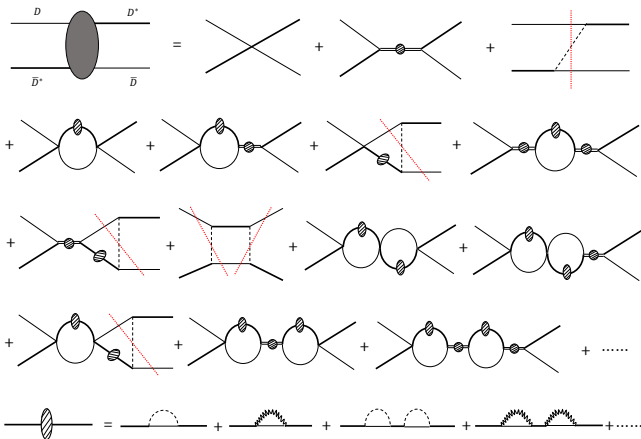


FIG. 3. The full scattering amplitudes of  $DD^* \rightarrow D\bar{D}^*$  in the coupled-channel dynamics. The self-energy diagram from the non-open-charm decays for the bare  $\chi'_{c1}$  is marked by shadow circle.

Firstly we do not consider the isospin violation of the contact interaction, i.e.,  $V_{ct}^{I=1} = 0 \text{ GeV}^{-2}$ . The solved observable pole structures and the corresponding component possibilities are listed in Table I. For different cutoff  $\lambda$ , one can adjust the  $V_{ct}^{I=0}$  to reproduce the small binding energy of  $X(3872)$ , and it can be seen that the pole width of  $X(3872)$  is still small if the non-open-charm decays of the bare  $\chi'_{c1}$  are not considered. When involving the width  $\Gamma_a + \Gamma_b$  from the bare state, its decay dynamics can be transferred into other poles by the coupled-channel mechanism, which significantly enlarges the pole width of  $X(3872)$  to the order of  $\mathcal{O}(10^{-1})$  MeV. Therefore, the accurate pole width of  $X(3872)$  can actually be treated as a novel indicator to convincingly probe the role of the coupled-channel dynamics in the  $DD^*$  scattering.

As a prediction, there is indeed a higher resonance pole around 4 GeV, which could correspond to the genuine dressed charmonium  $\chi'_{c1}$  resonance as argued in Refs. [73–79] or a distorted  $DD^*$  resonance, in the case that the bare  $\chi'_{c1}$  resonance has evolved into a virtual pole far from the physical area in the  $(-, -)$  sheet. Furthermore, we find that the pole width of  $X(3872)$  and the properties of the new resonance significantly depend on the cutoff  $\lambda$ , which embodies the strong or weak coupling modes mentioned in the above section. For example, it can be identified that the  $X(3872)$  pole originates from the shadow resonance of  $\chi'_{c1}$  in the  $(-, +)$  sheet for  $\lambda = 0.5 \text{ GeV}^{-1}$  or the  $DD^*$  pole in the  $(-, +)$  sheet for  $\lambda = 2.5 \text{ GeV}^{-1}$ , which correspond to the strong or weak coupling mode, respectively. Thus, the precise measurement of  $X(3872)$  and the search for the missing higher charmonium-like resonance might provide a strong limitation and reveal the dynamical origin and nature of  $X(3872)$ . The results assuming an evident isospin violation of the contact interaction are summarized in Appendix, in which the similar conclusions are obtained.

*Summary.*— We have studied the pole origin of  $X(3872)$  with the coupled-channel dynamics involving the interaction

between the first excited  $P$ -wave charmonium core and the  $DD^*$  continuum channels and definitely demonstrated that the  $X(3872)$  does not originate from the mass shift of the bare  $\chi'_{c1}$  resonance pole. Accordingly, it stems from either the  $DD^*$  virtual state pole in the weak-coupling mode or the shadow pole associated with  $\chi'_{c1}$  in the strong-coupling mode. Furthermore, we focused on the pole width of  $X(3872)$  by considering the complete scattering dynamics, which is implemented by the complete scaling method. Here, three important dynamical mechanisms including the three-body threshold effect from the OPE potential, the dynamical width of  $\bar{D}^*$  and the non-open-charm decays of the bare  $\chi'_{c1}$  state are considered to produce the pole width. Our findings indicate that the coupled-channel dynamics will result in an apparently larger pole width of  $X(3872)$ . In addition, we have established a quantitative connection among the dynamical origin of  $X(3872)$ , its pole width and the properties of the predicted new resonance. We emphasize that the precise measurement of the pole width of  $X(3872)$  and the search for the higher charmoniumlike resonance should be very significant for thoroughly solving the puzzle of  $X(3872)$ , which shall hopefully be achieved with the forthcoming upgrade of LHCb, BESIII and Belle II.

## ACKNOWLEDGEMENTS

This work is supported by the National Science Foundation of China under Grants No. 11975033, No. 12070131001 and No. 12147168. This project was also funded by the Deutsche Forschungsgemeinschaft (DFG, German Research Foundation, Project ID 196253076-TRR 110). J.Z.W. is also supported by the National Postdoctoral Program for Innovative Talent.

## APPENDIX

### The uniformization in the two-channel problem

For the two-channel threshold  $m_{th0}$  and  $m_{th\pm}$ , we define two momentum-like variables

$$p_0^2 = E^2 - m_{th0}^2, \quad p_{\pm}^2 = E^2 - m_{th\pm}^2, \quad (11)$$

and  $p_{\pm}^2 - p_0^2 = \Delta^2$ . The operation mapping  $E$  to  $z$  is given by the following relations,

$$p_{\pm} + p_0 = \Delta z, \quad p_0 - p_{\pm} = \frac{\Delta}{z}. \quad (12)$$

Based on the definition of the variable  $z$ , the same energy  $E$  in four different Riemann sheets can be mapped onto different regions in the  $z$ -plane, which is the so-called uniformization process. Here, the origin of the  $z$ -plane is mapped to the infinity of the  $(-, +)$  and  $(+, -)$  Riemann sheets, so the molecular pole and the  $\chi'_{c1}$  state stem from the origin and the real axis, respectively.

TABLE I. The poles and component possibilities of  $X(3872)$  and a new resonance in the complete coupled-channel dynamics. The pole of  $X(3872)$  is given by the binding energy relative to the  $D^0\bar{D}^{*0}$  threshold. The  $\chi$  and  $M$  superscripts denote the dressed  $\chi'_{c1}$  resonance and the distorted  $D\bar{D}^*$  resonance in the  $(-, -)$  sheet, respectively. Here,  $V_{ct}^{I=1} = 0 \text{ GeV}^{-2}$  and all pole positions are in units of MeV.

$\lambda(V_{ct}^{I=0}) \text{ GeV}^{-1} (\text{GeV}^{-2})$			0.5 (96.6)	1.0 (22.5)	1.25 (11.2)	1.5 (3.7)	2.5 (-13.1)
Without $\Gamma_a + \Gamma_b$	$X(3872)$	Pole	-0.086-0.003i	-0.140-0.024i	-0.097-0.027i	-0.089-0.029i	-0.075-0.030i
With $\Gamma_a + \Gamma_b$	$X(3872)$	Pole	-0.059-1.36i	-0.060-0.293i	-0.060-0.164i	-0.070-0.119i	-0.071-0.065i
		$\mathcal{P}_{D^0\bar{D}^{*0}}$	0.145-0.015i	0.748-0.136i	0.858-0.078i	0.895-0.047i	0.939-0.013i
		$\mathcal{P}_{D^+\bar{D}^{*-}}$	0.110+0.002i	0.092+0.049i	0.065+0.035i	0.056+0.024i	0.043+0.009i
		$\mathcal{P}_{\chi'_{c1}}$	0.745+0.013i	0.160+0.087i	0.077+0.043i	0.049+0.023i	0.018+0.004i
	New resonance	Pole	4150-141i <sup>M</sup>	4063-129i <sup>M</sup>	4025-92i <sup>\chi</sup>	4004-57i <sup>\chi</sup>	3977-8i <sup>\chi</sup>
		$\mathcal{P}_{D^0\bar{D}^{*0}}$	0.328+0.048i	0.278-0.191i	0.203-0.255i	0.104-0.209i	0.088-0.040i
		$\mathcal{P}_{D^+\bar{D}^{*-}}$	0.324+0.007i	0.265-0.219i	0.187-0.286i	0.086-0.234i	0.092-0.062i
		$\mathcal{P}_{\chi'_{c1}}$	0.348-0.055i	0.457+0.410i	0.610+0.541i	0.810+0.443i	0.820+0.102i
BESIII [64]	Pole	$(0.0068^{+0.1655}_{-0.1700}) - (0.190^{+0.206}_{-0.161})i$					
LHCb [63]	Pole	$(0.06^{+0.16}_{-0.16}) - (0.13^{+0.32}_{-0.18})i$					

### The non-open charm and open charm decay behaviors of bare $P$ -wave charmonium $\chi'_{c1}$

The important non-open charm decays of the  $c\bar{c}$  state include the light hadron decay and the radiative transition into the lower charmoniums. For a  $n^3P_1$  charmonium, its inclusive decays to various light hadron final states mainly occur through the annihilation process  $n^3P_1 \rightarrow q\bar{q}g$ , whose width depends on the first-order derivative of its radial wave function at the origin [80],

$$\Gamma(n^3P_1 \rightarrow q\bar{q}g) = \frac{32\alpha_s^3}{9\pi m_c^4} |R'_{nP}(0)|^2 \ln(m_c \langle R \rangle), \quad (13)$$

where  $\langle R \rangle$  is the average radius of the  $n^3P_1$  state,  $m_c = 1.65 \text{ GeV}$  and  $\alpha_s = 0.26$ . For the radiative decays of the charmonium, the partial width of the  $E1$  transition  $n^{2S+1}L_J \rightarrow n'^{2S'+1}L'_{J'}\gamma$  is given by [81],

$$\Gamma_{E1} = \frac{4}{3} \alpha e_c^2 \omega^3 \delta_{L,L'\pm 1} C_{if} |\langle \psi_f | r | \psi_i \rangle|^2, \quad (14)$$

with

$$C_{if} = \max(L, L') (2J' + 1) \begin{Bmatrix} L' & J' & S \\ J & L & 1 \end{Bmatrix}^2, \quad (15)$$

where the  $e_c$  is the charm quark charge in units of  $|e|$ ,  $\alpha$  is the fine-structure constant,  $\omega$  is the emitted photon energy and  $\langle \psi_f | r | \psi_i \rangle = \int_0^\infty R_{n'L'}(r) r R_{nL}(r) r^2 dr$  is the transition matrix element. The partial width of the  $M1$  radiative transition

$n^{2S+1}L_J \rightarrow n'^{2S'+1}L'_{J'}\gamma$  with the spin flip can be written as [82]

$$\Gamma_{M1} = \frac{4\alpha e_c^2 \omega^3}{3m_c^2} \delta_{S,S'\pm 1} \frac{2J'+1}{2L+1} \left| \langle \psi_f | j_0\left(\frac{\omega r}{2}\right) | \psi_i \rangle \right|^2, \quad (16)$$

with

$$\langle \psi_f | j_0\left(\frac{\omega r}{2}\right) | \psi_i \rangle = \int_0^\infty R_{n'L'}(r) j_0\left(\frac{\omega r}{2}\right) R_{nL}(r) r^2 dr, \quad (17)$$

where  $j_0(\frac{\omega r}{2})$  is the spherical Bessel function. For the first excited  $P$ -wave charmonium  $\chi'_{c1}$ , the kinematically allowed final states of  $E1$  transition include  $J/\psi\gamma$ ,  $\psi(3686)\gamma$ ,  $\psi(3770)\gamma$  and  $\psi_2(3823)\gamma$ , and the corresponding  $M1$  transition process is  $\chi'_{c1} \rightarrow h_c\gamma$ .

The quark pair creation (QPC) model is a very successful phenomenological approach in depicting the two-body OZI-allowed strong decay behaviors covering the light meson to heavy quarkonium system [83, 84]. The QPC model assumes that the quark-antiquark pair  $q\bar{q}$  created from the vacuum is a  $^3P_0$  state with the spin-parity  $J^{PC} = 0^{++}$ , and the transition operators  $\mathcal{T}$  can be expressed as

$$\begin{aligned} \mathcal{T} = & -3\gamma \sum_m \langle 1m; 1-m | 00 \rangle \int d\mathbf{p}_3 d\mathbf{p}_4 \delta^3(\mathbf{p}_3 + \mathbf{p}_4) \\ & \times \mathcal{Y}_{1m} \left( \frac{\mathbf{p}_3 - \mathbf{p}_4}{2} \right) \chi_{1,-m}^{34} \phi_0^{34} \omega_0^{34} b_{3i}^\dagger(\mathbf{p}_3) d_{4j}^\dagger(\mathbf{p}_4), \end{aligned} \quad (18)$$

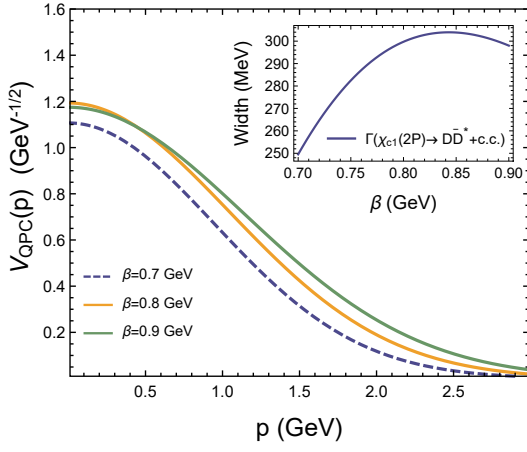


FIG. 4. The numerical  $\mathcal{V}_{0j}(\mathbf{q})$  between the bare  $\chi'_{c1}$  and the  $D^0\bar{D}^{*0}/D^+\bar{D}^{*-}$  continuum and the corresponding open-charm decay width in the QPC model.

where  $\mathcal{Y}_{lm}(\mathbf{p}) = p^l Y_{lm}(\theta_p, \phi_p)$ ,  $b_3^\dagger(d_4^\dagger)$  is the quark (anti-quark) creation operator, and  $\phi_0^{34} = (u\bar{u} + d\bar{d} + s\bar{s})/\sqrt{3}$  and  $\omega_0^{34}$  are SU(3) flavor and color wave function of vacuum quark pair, respectively. The dimensionless parameter  $\gamma^2$ , reflecting the strength of the vacuum quark pair creation, has been determined as  $40.9 \pm 8.2$  in Ref. [66] for the charmonium family. The transition amplitude of  $\chi'_{c1} \rightarrow D\bar{D}^*$  is

$$\mathcal{M} = \langle D\bar{D}^* | \mathcal{T} | \chi'_{c1} \rangle, \quad (19)$$

which is proportional to the overlap integral of the wave functions in momentum space

$$I(\mathbf{q}) = \int d^3\mathbf{p} \Psi_{n_A L_A M_L A}(\mathbf{q} + \mathbf{p}) \Psi_{n_B L_B M_L B}^* \left( \frac{m_q \mathbf{q}}{m_c + m_q} + \mathbf{p} \right) \times \mathcal{Y}_{lm}(\mathbf{p}) \Psi_{n_C L_C M_L C}^* \left( \frac{m_q \mathbf{q}}{m_{\bar{c}} + m_q} + \mathbf{p} \right), \quad (20)$$

where  $\mathbf{q}$  denotes the momentum of either outgoing charmed meson, and  $\Psi_{n_L M_L}(\mathbf{p})$  is the spatial wave function, while the notation  $A$ ,  $B$  and  $C$  refer to the  $\chi'_{c1}$ ,  $D$  and  $\bar{D}^*$  states, respectively. It is worth emphasizing that the overlap integral  $I(\mathbf{q})$  provides the momentum-dependent part of the  $\mathcal{V}_{0j}(\mathbf{q})$  and  $\mathcal{V}_{i0}(\mathbf{q}')$  in Eq. (6).

The numerical coupled-channel interaction  $\mathcal{V}_{0j}(\mathbf{q})$  between the bare  $\chi'_{c1}$  and the  $D^0\bar{D}^{*0}/D^+\bar{D}^{*-}$  continuum estimated by the QPC model is shown in Fig. 4 with  $\beta = 0.7, 0.8$  and  $0.9$  GeV.  $\beta$  is a quantity reflecting the wave function distribution of  $\chi'_{c1}$ . We also illustrate the variation of the total decay width of  $\chi'_{c1} \rightarrow D\bar{D}^* + c.c.$  with  $\beta$ , which is estimated to be  $250 \sim 320$  MeV. Such a large decay width also implies that the  $s$ -channel coupling with the  $D\bar{D}^*$  may be too strong to be ignored. Based on the same range of  $\beta$ , the estimated widths of the radiative transitions and inclusive light hadron decays of the bare  $\chi'_{c1}$  are presented in Fig. 5. It can be seen that the  $\psi(3686)\gamma$  is the dominant radiative decay mode although its phase space is far smaller than that of  $J/\psi\gamma$ , which mainly benefits from the node effect from

the wave function overlap. Additionally, the  $\psi(3770)\gamma$  and  $\psi_2(3823)\gamma$  are also important radiative modes, whose widths are  $10 \sim 20$  keV. The  $\Gamma(\chi'_{c1} \rightarrow q\bar{q}g)$  can reach  $2.6 \sim 7.6$  MeV, which should govern the non-open-charm decays of the bare  $\chi'_{c1}$ . If assuming the  $D\bar{D}^*$  component of  $X(3872)$  does not decay to  $\psi(3686)\gamma$  and  $J/\psi\gamma$ , the theoretical value of the ratio  $R = \Gamma(\psi(3686)\gamma)/\Gamma(J/\psi\gamma)$  including the phase space correction coincides with the corresponding experimental values from the Belle and LHCb Collaboration [85, 86] within a narrower range of  $\beta = 0.73 \sim 0.766$  GeV.

### The three-body $D\bar{D}\pi$ threshold dynamics and the self-energy effect of $\bar{D}^*$ in the $D\bar{D}^*$ scattering

A typical OPE potential  $V_\pi$  of the  $[D\bar{D}^*]_i \rightarrow [D\bar{D}^*]_j$  can be written as

$$V_\pi^{ij}(q, q', z) = \frac{g^2}{4f_\pi^2} \frac{(\boldsymbol{\varepsilon} \cdot \mathbf{p})(\boldsymbol{\varepsilon}' \cdot \mathbf{p})}{p_0^2 - (q^2 + q'^2 - 2qq'z) - m_\pi^2 + i\epsilon}, \quad (21)$$

where  $i(j) = 1, 2$  stands for  $[D^0\bar{D}^{*0}]$  and  $[D^+\bar{D}^{*-}]$ , respectively, and the  $p$  is defined as the four-momentum ( $p_1$ - $p_4$ ) of the exchanged pion, and  $p_1, p_2, p_3$  and  $p_4$  correspond to the four-momentum of the initial charmed meson  $D, \bar{D}^*$  and final charmed meson  $\bar{D}$  and  $D^*$ , respectively. The  $q(q')$  and  $z$  denote the magnitudes of the three-momentum  $\mathbf{p}_1(\mathbf{p}_4)$  and the cosine of the angle between  $\mathbf{p}_1$  and  $\mathbf{p}_4$ , respectively. The coupling constant  $g = 0.53$  [59] and pion decay constant  $f_\pi = 0.086$  [28]. Since the  $p_0 \sim (m_{D^*} - m_D) > m_\pi^{\text{phy}}$  will lead to an on-shell pion exchange, the  $D\bar{D}^*$  system couples to the three-body channel of  $D\bar{D}\pi$ . In order to include this three-body threshold effect, the OPE potential can be modified as [28]

$$V_\pi^{ij}(q, q', z) = \frac{g^2}{4f_\pi^2} \frac{(\boldsymbol{\varepsilon} \cdot \mathbf{p})(\boldsymbol{\varepsilon}' \cdot \mathbf{p})}{(E' + \delta_{ij})^2 - (q^2 + q'^2 - 2qq'z) - m_\pi^2 + i\epsilon} \quad (22)$$

where the system energy  $E$  is the sum of the center-of-mass kinetic energy  $E' = k_0^2/(2\mu)$  and the lowest two-body threshold  $m_{D^0} + m_{\bar{D}^{*0}}$ , and  $\delta_{11} = m_{D^{*0}} - m_{D^0}$ ,  $\delta_{12} = m_{D^{*0}} - m_{D^+}$ ,  $\delta_{21} = m_{D^{*0}} - m_{D^+}$  and  $\delta_{22} = m_{D^{*0}} + m_{D^0} - 2m_{D^+}$ . Here, for the concerned poles near the two-body threshold, ignoring the kinetic energy of the heavy meson is a good approximation. When considering the kinetic energy term of heavy meson, Eq. (22) can be further revised by the following replacement of  $\delta \rightarrow \delta - (p^2 + p'^2)/(2m_D)$ . More discussions and applications of the three-body threshold effects can be found in Refs. [28, 39].

The matrix form of the contact interaction of the  $D\bar{D}^*$  scattering reads

$$V_{\text{contact}} = \begin{pmatrix} C_t & C'_t \\ C'_t & C_t \end{pmatrix}. \quad (23)$$

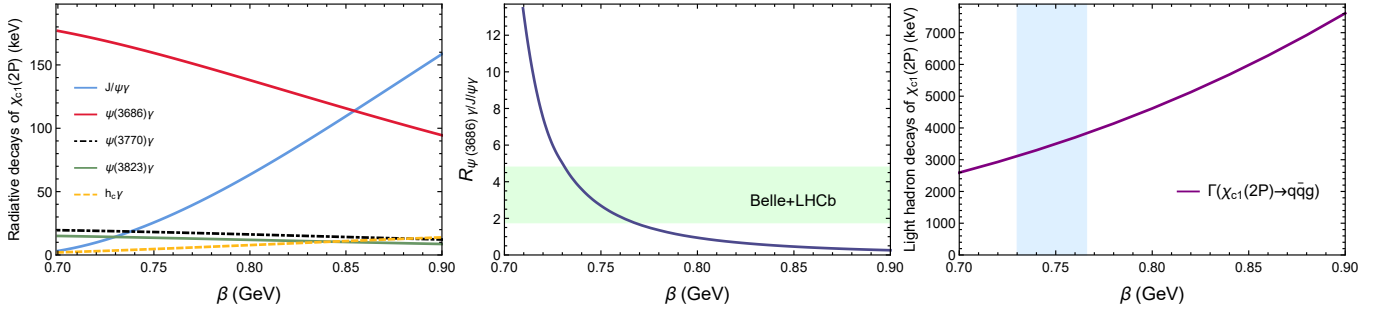


FIG. 5. Theoretical widths of the radiative transitions and inclusive light hadrons decays of the bare  $\chi'_{c1}$  state.

We define two new leading-order low-energy coupling constant  $V_{ct}^{I=0}$  and  $V_{ct}^{I=1}$ , which can be related to  $C_t$  and  $C'_t$  by

$$\begin{aligned} C_t &= \frac{1}{2}(V_{ct}^{I=0} + V_{ct}^{I=1}), \\ C'_t &= \frac{1}{2}(V_{ct}^{I=0} - V_{ct}^{I=1}). \end{aligned} \quad (24)$$

Here, the  $I$  represents the isospin of the  $D\bar{D}^*$  system.

Because the  $D^{*0}$  and  $D^{*\pm}$  have comparable widths with the pole width of  $X(3872)$ , it is necessary to take into account the width for the propagator of  $D^*$  [27], which includes both the intermediate  $\bar{D}\pi$  and  $\bar{D}\gamma$  self-energy diagrams and is different from the mechanism of the revised OPE potential with the three-body threshold cut. The real part of the self-energy of  $D^*$  is approximately absorbed into the physical mass of the  $D^*$  meson. The imaginary part of the self-energy of  $D^*$  is given by

$$\begin{aligned} \Gamma_{D^{*+}}(E) &= \frac{g^2 m_{D^0}}{12\pi f_\pi^2 m_{D^{*+}}} k_{D^0\pi^+}^3 + \frac{g^2 m_{D^+}}{24\pi f_\pi^2 m_{D^{*+}}} k_{D^+\pi^0}^3 \\ &\quad + \Gamma(D^{*+} \rightarrow D^+\gamma), \\ \Gamma_{D^{*0}}(E) &= \frac{g^2 m_{D^0}}{24\pi f_\pi^2 m_{D^{*0}}} k_{D^0\pi^0}^3, \end{aligned} \quad (25)$$

where the  $D^*$  width is treated as a function of the center-of-mass energy  $E$  rather than a constant since the  $D^*$  is not always on-shell in the complex energy space. Consequently, the the width of  $D^*$  can be introduced into the scattering dynamics by modifying the Schrödinger equation as [28]

$$E\phi(\mathbf{p}) = \left(\frac{\mathbf{p}^2}{2\mu} - i\frac{\Gamma(E)}{2}\right)\phi(\mathbf{p}) + \int \frac{d^3\mathbf{k}}{(2\pi)^3} V(\mathbf{p}, \mathbf{k})\phi(\mathbf{k}), \quad (26)$$

where  $\frac{\mathbf{p}^2}{2\mu} - i\frac{\Gamma(E)}{2}$  means a modified kinetic energy term for the unstable system.

#### The pole behaviors of the full $D\bar{D}^*$ scattering dynamics by considering the isospin violation of the contact potential

Considering the full  $D\bar{D}^*$  scattering dynamics and the evident isospin violation of the contact interaction, the pole be-

haviors of the  $X(3872)$  and the new resonance are summarized in Table II and Table III, which correspond to  $V_{ct}^{I=1} = 30 \text{ GeV}^{-2}$  and  $V_{ct}^{I=1} = -30 \text{ GeV}^{-2}$ , respectively. Interestingly, there almost exists a one-to-one correspondence between the cutoff  $\lambda$  and the pole imaginary of the new charmoniumlike resonance, which almost does not depend on the contact potential  $V_{ct}^{I=1}$ .

Furthermore, it can be seen that the isospin violation impact on  $X(3872)$  is obviously greater than that on the dressed  $\chi'_{c1}$  resonance or the distorted  $D\bar{D}^*$  resonance. This feature can explain the absence of the experimental signal of this higher charmoniumlike resonance in the final states of  $J/\psi\pi^+\pi^-$  [59], which is a typical isospin violation channel of discovering the  $X(3872)$ . Additionally, if adopting the center value of the pole width of  $X(3872)$  measured by the BESIII and LHCb Collaborations [63, 64] as inputs, the pole width of the new charmoniumlike resonance is predicted to be around 100 MeV, and such a large width might explain why this state is still missing in experiments.

\* wangjzh2022@pku.edu.cn

† lzy\_15@pku.edu.cn

‡ chenyank@stu.pku.edu.cn

§ lu.meng@rub.de

¶ zhushl@pku.edu.cn

- [1] H.-X. Chen, W. Chen, X. Liu, and S.-L. Zhu, The hidden-charm pentaquark and tetraquark states, *Phys. Rept.* **639**, 1 (2016), arXiv:1601.02092 [hep-ph].
- [2] Y.-R. Liu, H.-X. Chen, W. Chen, X. Liu, and S.-L. Zhu, Pentaquark and Tetraquark states, *Prog. Part. Nucl. Phys.* **107**, 237 (2019), arXiv:1903.11976 [hep-ph].
- [3] F.-K. Guo, C. Hanhart, U.-G. Meißner, Q. Wang, Q. Zhao, and B.-S. Zou, Hadronic molecules, *Rev. Mod. Phys.* **90**, 015004 (2018), [Erratum: Rev.Mod.Phys. 94, 029901 (2022)], arXiv:1705.00141 [hep-ph].
- [4] N. Brambilla, S. Eidelman, C. Hanhart, A. Nefediev, C.-P. Shen, C. E. Thomas, A. Vairo, and C.-Z. Yuan, The XYZ states: experimental and theoretical status and perspectives, *Phys. Rept.* **873**, 1 (2020), arXiv:1907.07583 [hep-ex].
- [5] S. L. Olsen, T. Skwarnicki, and D. Zieminska, Nonstandard heavy mesons and baryons: Experimental evidence, *Rev. Mod. Phys.* **90**, 015003 (2018), arXiv:1708.04012 [hep-ph].

TABLE II. The poles and component possibilities of  $X(3872)$  and a new resonance in the complete coupled-channel dynamics. The pole of  $X(3872)$  is given by the binding energy relative to the  $D^0\bar{D}^{*0}$  threshold. The  $\chi$  and  $M$  superscripts denote the dressed  $\chi'_{c1}$  resonance and the distorted  $D\bar{D}^*$  resonance in the  $(-, -)$  sheet, respectively. Here,  $V_{ct}^{I=1} = 30 \text{ GeV}^{-2}$  and all pole positions are in units of MeV.

$\lambda (V_{ct}^{I=0}) \text{ GeV}^{-1} (\text{GeV}^{-2})$			0.5 (96.4)	1.0 (21.8)	1.25 (10.3)	1.5 (2.7)	2.5 (-14.4)
With $\Gamma_a + \Gamma_b$	$X(3872)$	Pole	-0.077-1.37i	-0.064-0.333i	-0.066-0.189i	-0.074-0.133i	-0.075-0.069i
		$\mathcal{P}_{D^0\bar{D}^{*0}}$	0.138-0.010i	0.681-0.148i	0.809-0.095i	0.858-0.061i	0.916-0.018i
		$\mathcal{P}_{D^+\bar{D}^{*-}}$	0.116+0.000i	0.130+0.057i	0.098+0.047i	0.083+0.034i	0.063+0.013i
		$\mathcal{P}_{\chi'_{c1}}$	0.746+0.010i	0.189+0.091i	0.093+0.048i	0.059+0.027i	0.021+0.005i
	New resonance	Pole	4149-141i <sup>M</sup>	4061-129i <sup>M</sup>	4023-92i <sup>\chi</sup>	4004-56i <sup>\chi</sup>	3977-8i <sup>\chi</sup>
		$\mathcal{P}_{D^0\bar{D}^{*0}}$	0.324+0.054i	0.263-0.181i	0.205-0.230i	0.133-0.198i	0.082-0.037i
		$\mathcal{P}_{D^+\bar{D}^{*-}}$	0.328+0.001i	0.273-0.236i	0.154-0.335i	0.070-0.226i	0.073-0.055i
		$\mathcal{P}_{\chi'_{c1}}$	0.348-0.055i	0.464+0.417i	0.641+0.565i	0.797+0.424i	0.845+0.092i

TABLE III. The poles and component possibilities of  $X(3872)$  and a new resonance in the complete coupled-channel dynamics. The pole of  $X(3872)$  is given by the binding energy relative to the  $D^0\bar{D}^{*0}$  threshold. The  $\chi$  and  $M$  superscripts denote the dressed  $\chi'_{c1}$  resonance and the distorted  $D\bar{D}^*$  resonance in the  $(-, -)$  sheet, respectively. Here,  $V_{ct}^{I=1} = -30 \text{ GeV}^{-2}$  and all pole positions are in units of MeV.

$\lambda (V_{ct}^{I=0}) \text{ GeV}^{-1} (\text{GeV}^{-2})$			0.5 (97.0)	1.0 (25.4)	1.25 (14.6)	1.5 (7.7)	2.5 (-8.0)
With $\Gamma_a + \Gamma_b$	$X(3872)$	Pole	-0.064-1.32i	-0.067-0.178i	-0.078-0.113i	-0.073-0.084i	-0.076-0.055i
		$\mathcal{P}_{D^0\bar{D}^{*0}}$	0.170-0.041i	0.905-0.067i	0.946-0.027i	0.964-0.013i	0.982-0.003i
		$\mathcal{P}_{D^+\bar{D}^{*-}}$	0.092+0.009i	0.015+0.014i	0.010+0.006i	0.008+0.003i	0.006+0.001i
		$\mathcal{P}_{\chi'_{c1}}$	0.738+0.032i	0.085+0.053i	0.044+0.021i	0.028+0.010i	0.012+0.002i
	New resonance	Pole	4150-141i <sup>M</sup>	4066-127i <sup>M</sup>	4031-94i <sup>\chi</sup>	4008-60i <sup>\chi</sup>	3978-9i <sup>\chi</sup>
		$\mathcal{P}_{D^0\bar{D}^{*0}}$	0.329+0.043i	0.284-0.182i	0.230-0.258i	0.135-0.228i	0.075-0.056i
		$\mathcal{P}_{D^+\bar{D}^{*-}}$	0.323+0.011i	0.269-0.197i	0.217-0.271i	0.129-0.243i	0.081-0.073i
		$\mathcal{P}_{\chi'_{c1}}$	0.348-0.054i	0.447+0.379i	0.553+0.529i	0.736+0.471i	0.844+0.129i

- [6] L. Meng, B. Wang, G.-J. Wang, and S.-L. Zhu, Chiral perturbation theory for heavy hadrons and chiral effective field theory for heavy hadronic molecules, *Phys. Rept.* **1019**, 1 (2023), [arXiv:2204.08716 \[hep-ph\]](#).
- [7] S. K. Choi *et al.* (Belle), Observation of a narrow charmonium-like state in exclusive  $B^\pm \rightarrow K^\pm \pi^+ \pi^- J/\psi$  decays, *Phys. Rev. Lett.* **91**, 262001 (2003), [arXiv:hep-ex/0309032](#).
- [8] G. Gokhroo *et al.* (Belle), Observation of a Near-threshold  $D^0\bar{D}^0\pi^0$  Enhancement in  $B \rightarrow D^0\bar{D}^0\pi^0 K$  Decay, *Phys. Rev. Lett.* **97**, 162002 (2006), [arXiv:hep-ex/0606055](#).
- [9] M. B. Voloshin, Interference and binding effects in decays of possible molecular component of  $X(3872)$ , *Phys. Lett. B* **579**, 316 (2004), [arXiv:hep-ph/0309307](#).
- [10] E. Braaten and M. Kusunoki, Low-energy universality and the new charmonium resonance at 3870-MeV, *Phys. Rev. D* **69**, 074005 (2004), [arXiv:hep-ph/0311147](#).
- [11] E. S. Swanson, Short range structure in the  $X(3872)$ , *Phys. Lett. B* **588**, 189 (2004), [arXiv:hep-ph/0311229](#).
- [12] N. A. Tornqvist, Isospin breaking of the narrow charmonium state of Belle at 3872-MeV as a deuson, *Phys. Lett. B* **590**, 209 (2004), [arXiv:hep-ph/0402237](#).
- [13] S. Fleming, M. Kusunoki, T. Mehen, and U. van Kolck, Pion interactions in the  $X(3872)$ , *Phys. Rev. D* **76**, 034006 (2007), [arXiv:hep-ph/0703168](#).
- [14] Y.-R. Liu, X. Liu, W.-Z. Deng, and S.-L. Zhu, Is  $X(3872)$  Really a Molecular State?, *Eur. Phys. J. C* **56**, 63 (2008), [arXiv:0801.3540 \[hep-ph\]](#).
- [15] R. Aaij *et al.* (LHCb), Observation of an exotic narrow doubly charmed tetraquark, *Nature Phys.* **18**, 751 (2022), [arXiv:2109.01038 \[hep-ex\]](#).

- [16] R. Aaij *et al.* (LHCb), Study of the doubly charmed tetraquark  $T_{cc}^+$ , *Nature Commun.* **13**, 3351 (2022), arXiv:2109.01056 [hep-ex].
- [17] A. V. Manohar and M. B. Wise, Exotic Q Q anti-q anti-q states in QCD, *Nucl. Phys. B* **399**, 17 (1993), arXiv:hep-ph/9212236.
- [18] D. Janc and M. Rosina, The  $T_{cc} = DD^*$  molecular state, *Few Body Syst.* **35**, 175 (2004), arXiv:hep-ph/0405208.
- [19] S. Ohkoda, Y. Yamaguchi, S. Yasui, K. Sudoh, and A. Hosaka, Exotic mesons with double charm and bottom flavor, *Phys. Rev. D* **86**, 034019 (2012), arXiv:1202.0760 [hep-ph].
- [20] N. Li, Z.-F. Sun, X. Liu, and S.-L. Zhu, Coupled-channel analysis of the possible  $D^{(*)}D^{(*)}$ ,  $\bar{B}^{(*)}\bar{B}^{(*)}$  and  $D^{(*)}\bar{B}^{(*)}$  molecular states, *Phys. Rev. D* **88**, 114008 (2013), arXiv:1211.5007 [hep-ph].
- [21] K. Chen, R. Chen, L. Meng, B. Wang, and S.-L. Zhu, Systematics of the heavy flavor hadronic molecules, *Eur. Phys. J. C* **82**, 581 (2022), arXiv:2109.13057 [hep-ph].
- [22] X.-K. Dong, F.-K. Guo, and B.-S. Zou, A survey of heavy-heavy hadronic molecules, *Commun. Theor. Phys.* **73**, 125201 (2021), arXiv:2108.02673 [hep-ph].
- [23] A. Feijoo, W. H. Liang, and E. Oset,  $D^0 D^0 \pi^+$  mass distribution in the production of the  $T_{cc}$  exotic state, *Phys. Rev. D* **104**, 114015 (2021), arXiv:2108.02730 [hep-ph].
- [24] M. Albaladejo, Tcc+ coupled channel analysis and predictions, *Phys. Lett. B* **829**, 137052 (2022), arXiv:2110.02944 [hep-ph].
- [25] S. Fleming, R. Hodges, and T. Mehen,  $T_{cc}^+$  decays: Differential spectra and two-body final states, *Phys. Rev. D* **104**, 116010 (2021), arXiv:2109.02188 [hep-ph].
- [26] L. Meng, G.-J. Wang, B. Wang, and S.-L. Zhu, Probing the long-range structure of the  $T_{cc}^+$  with the strong and electromagnetic decays, *Phys. Rev. D* **104**, 051502 (2021), arXiv:2107.14784 [hep-ph].
- [27] M.-L. Du, V. Baru, X.-K. Dong, A. Filin, F.-K. Guo, C. Hanhart, A. Nefediev, J. Nieves, and Q. Wang, Coupled-channel approach to Tcc+ including three-body effects, *Phys. Rev. D* **105**, 014024 (2022), arXiv:2110.13765 [hep-ph].
- [28] Z.-Y. Lin, J.-B. Cheng, and S.-L. Zhu,  $T_{cc}^+$  and  $X(3872)$  with the complex scaling method and  $DD(\bar{D})\pi$  three-body effect, (2022), arXiv:2205.14628 [hep-ph].
- [29] J.-B. Cheng, Z.-Y. Lin, and S.-L. Zhu, Double-charm tetraquark under the complex scaling method, *Phys. Rev. D* **106**, 016012 (2022), arXiv:2205.13354 [hep-ph].
- [30] H.-W. Ke, X.-H. Liu, and X.-Q. Li, Possible molecular states of  $D^{(*)}D^{(*)}$  and  $B^{(*)}B^{(*)}$  within the Bethe-Salpeter framework, *Eur. Phys. J. C* **82**, 144 (2022), arXiv:2112.14142 [hep-ph].
- [31] X.-Z. Ling, M.-Z. Liu, L.-S. Geng, E. Wang, and J.-J. Xie, Can we understand the decay width of the  $T_{cc}^+$  state?, *Phys. Lett. B* **826**, 136897 (2022), arXiv:2108.00947 [hep-ph].
- [32] Y. Liu, M. A. Nowak, and I. Zahed, Holographic tetraquarks and the newly observed  $T_{cc}^+$  at LHCb, *Phys. Rev. D* **105**, 054021 (2022), arXiv:1909.02497 [hep-ph].
- [33] M.-J. Yan and M. P. Valderrama, Subleading contributions to the decay width of the  $T_{cc}^+$  tetraquark, *Phys. Rev. D* **105**, 014007 (2022), arXiv:2108.04785 [hep-ph].
- [34] Y. Jin, S.-Y. Li, Y.-R. Liu, Q. Qin, Z.-G. Si, and F.-S. Yu, Color and baryon number fluctuation of preconfinement system in production process and  $T_{cc}$  structure, *Phys. Rev. D* **104**, 114009 (2021), arXiv:2109.05678 [hep-ph].
- [35] Q. Xin and Z.-G. Wang, Analysis of the doubly-charmed tetraquark molecular states with the QCD sum rules, *Eur. Phys. J. A* **58**, 110 (2022), arXiv:2108.12597 [hep-ph].
- [36] J. Shi, E. Wang, and Q. Wang, Investigating the isospin property of  $T_{cc}^+$  from its Dalitz plot distribution, *Phys. Rev. D* **106**, 096012 (2022), arXiv:2205.05234 [hep-ph].
- [37] P. G. Ortega, J. Segovia, D. R. Entem, and F. Fernandez, Nature of the doubly-charmed tetraquark  $T_{cc}^+$  in a constituent quark model, *Phys. Lett. B* **841**, 137918 (2023), [Erratum: Phys.Lett.B 847, 138308 (2023)], arXiv:2211.06118 [hep-ph].
- [38] M.-L. Du, A. Filin, V. Baru, X.-K. Dong, E. Epelbaum, F.-K. Guo, C. Hanhart, A. Nefediev, J. Nieves, and Q. Wang, Role of Left-Hand Cut Contributions on Pole Extractions from Lattice Data: Case Study for  $T_{cc}(3875)^+$ , *Phys. Rev. Lett.* **131**, 131903 (2023), arXiv:2303.09441 [hep-ph].
- [39] J.-Z. Wang, Z.-Y. Lin, and S.-L. Zhu, Cut structures and an observable singularity in the three-body threshold dynamics: the  $T_{cc}^+$  case, (2023), arXiv:2309.09861 [hep-ph].
- [40] B. Wang and L. Meng, Revisiting the  $DD^*$  chiral interactions with the local momentum-space regularization up to the third order and the nature of  $T_{cc}^+$ , *Phys. Rev. D* **107**, 094002 (2023), arXiv:2212.08447 [hep-ph].
- [41] C. Chen, C. Meng, Z. Xiao, and H.-Q. Zheng, Some remarks on compositeness of  $T_{cc}^+$ , *Chin. Phys. C* **48**, 043102 (2024), arXiv:2307.12069 [hep-ph].
- [42] R. Chen, Q. Huang, X. Liu, and S.-L. Zhu, Predicting another doubly charmed molecular resonance  $T_{cc}^{\prime+}(3876)$ , *Phys. Rev. D* **104**, 114042 (2021), arXiv:2108.01911 [hep-ph].
- [43] R. Aaij *et al.* (LHCb), Determination of the  $X(3872)$  meson quantum numbers, *Phys. Rev. Lett.* **110**, 222001 (2013), arXiv:1302.6269 [hep-ex].
- [44] R. Aaij *et al.* (LHCb), Quantum numbers of the  $X(3872)$  state and orbital angular momentum in its  $\rho^0 J/\psi$  decay, *Phys. Rev. D* **92**, 011102 (2015), arXiv:1504.06339 [hep-ex].
- [45] V. Baru, C. Hanhart, Y. S. Kalashnikova, A. E. Kudryavtsev, and A. V. Nefediev, Interplay of quark and meson degrees of freedom in a near-threshold resonance, *Eur. Phys. J. A* **44**, 93 (2010), arXiv:1001.0369 [hep-ph].
- [46] C. Hanhart, Y. S. Kalashnikova, and A. V. Nefediev, Interplay of quark and meson degrees of freedom in a near-threshold resonance: multi-channel case, *Eur. Phys. J. A* **47**, 101 (2011), arXiv:1106.1185 [hep-ph].
- [47] I. K. Hammer, C. Hanhart, and A. V. Nefediev, Remarks on meson loop effects on quark models, *Eur. Phys. J. A* **52**, 330 (2016), arXiv:1607.06971 [hep-ph].
- [48] C. Hanhart and A. Nefediev, Do near-threshold molecular states mix with neighboring  $Q\bar{Q}$  states?, *Phys. Rev. D* **106**, 114003 (2022), arXiv:2209.10165 [hep-ph].
- [49] M. R. Pennington and D. J. Wilson, Decay channels and charmonium mass-shifts, *Phys. Rev. D* **76**, 077502 (2007), arXiv:0704.3384 [hep-ph].
- [50] S. Ono and N. A. Tornqvist, Continuum Mixing and Coupled Channel Effects in  $c\bar{c}$  and  $b\bar{b}$  Quarkonium, *Z. Phys. C* **23**, 59 (1984).
- [51] B.-Q. Li, C. Meng, and K.-T. Chao, Coupled-Channel and Screening Effects in Charmonium Spectrum, *Phys. Rev. D* **80**, 014012 (2009), arXiv:0904.4068 [hep-ph].
- [52] Z.-Y. Zhou and Z. Xiao, Comprehending heavy charmonia and their decays by hadron loop effects, *Eur. Phys. J. A* **50**, 165 (2014), arXiv:1309.1949 [hep-ph].
- [53] M.-X. Duan, S.-Q. Luo, X. Liu, and T. Matsuki, Possibility of charmoniumlike state  $X(3915)$  as  $\chi_{c0}(2P)$  state, *Phys. Rev. D* **101**, 054029 (2020), arXiv:2002.03311 [hep-ph].
- [54] Q. Deng, R.-H. Ni, Q. Li, and X.-H. Zhong, Charmonia in an unquenched quark model, (2023), arXiv:2312.10296 [hep-ph].
- [55] Z.-L. Man, C.-R. Shu, Y.-R. Liu, and H. Chen, Charmonium states in a coupled-channel model, (2024), arXiv:2402.02765 [hep-ph].

- [56] J. A. Oller, E. Oset, and J. R. Pelaez, Meson meson interaction in a nonperturbative chiral approach, *Phys. Rev. D* **59**, 074001 (1999), [Erratum: *Phys.Rev.D* 60, 099906 (1999), Erratum: *Phys.Rev.D* 75, 099903 (2007)], [arXiv:hep-ph/9804209](#).
- [57] S. Godfrey and N. Isgur, Mesons in a Relativized Quark Model with Chromodynamics, *Phys. Rev. D* **32**, 189 (1985).
- [58] T. Barnes, S. Godfrey, and E. S. Swanson, Higher charmonia, *Phys. Rev. D* **72**, 054026 (2005), [arXiv:hep-ph/0505002](#).
- [59] R. L. Workman *et al.* (Particle Data Group), Review of Particle Physics, *PTEP* **2022**, 083C01 (2022).
- [60] W. Yamada and O. Morimatsu, New method to extract information of near-threshold resonances: Uniformized Mittag-Leffler expansion of Green's function and  $T$  matrix, *Phys. Rev. C* **102**, 055201 (2020), [arXiv:2005.07022 \[hep-ph\]](#).
- [61] W. A. Yamada, O. Morimatsu, T. Sato, and K. Yazaki, Near-threshold spectrum from a uniformized Mittag-Leffler expansion: Pole structure of the  $Z(3900)$ , *Phys. Rev. D* **105**, 014034 (2022), [arXiv:2108.11605 \[hep-ph\]](#).
- [62] L. Meng, B. Wang, and S.-L. Zhu, Double thresholds distort the line shapes of the  $P\psi\Lambda(4338)0$  resonance, *Phys. Rev. D* **107**, 014005 (2023), [arXiv:2208.03883 \[hep-ph\]](#).
- [63] R. Aaij *et al.* (LHCb), Study of the lineshape of the  $\chi_{c1}(3872)$  state, *Phys. Rev. D* **102**, 092005 (2020), [arXiv:2005.13419 \[hep-ex\]](#).
- [64] M. Ablikim *et al.* (BESIII), A coupled-channel analysis of the  $X(3872)$  lineshape with BESIII data, (2023), [arXiv:2309.01502 \[hep-ex\]](#).
- [65] F. E. Close and E. S. Swanson, Dynamics and decay of heavy-light hadrons, *Phys. Rev. D* **72**, 094004 (2005), [arXiv:hep-ph/0505206](#).
- [66] D. Guo, J.-Z. Wang, D.-Y. Chen, and X. Liu, Connection between near the  $D_s^+ D_s^-$  threshold enhancement in  $B^+ \rightarrow D_s^+ D_s^- K^+$  and conventional charmonium  $\chi_{c0}(2P)$ , *Phys. Rev. D* **106**, 094037 (2022), [arXiv:2210.16720 \[hep-ph\]](#).
- [67] D. Morel and S. Capstick, Baryon meson loop effects on the spectrum of nonstrange baryons, (2002), [arXiv:nucl-th/0204014](#).
- [68] P. G. Ortega, J. Segovia, D. R. Entem, and F. Fernandez, Molecular components in P-wave charmed-strange mesons, *Phys. Rev. D* **94**, 074037 (2016), [arXiv:1603.07000 \[hep-ph\]](#).
- [69] Z. Yang, G.-J. Wang, J.-J. Wu, M. Oka, and S.-L. Zhu, Novel Coupled Channel Framework Connecting the Quark Model and Lattice QCD for the Near-threshold  $D_s$  States, *Phys. Rev. Lett.* **128**, 112001 (2022), [arXiv:2107.04860 \[hep-ph\]](#).
- [70] J. Aguilar and J. M. Combes, A class of analytic perturbations for one-body schrodinger hamiltonians, *Commun. Math. Phys.* **22**, 269 (1971).
- [71] E. Balslev and J. M. Combes, Spectral properties of many-body schrodinger operators with dilatation-analytic interactions, *Commun. Math. Phys.* **22**, 280 (1971).
- [72] T. Myo, Y. Kikuchi, H. Masui, and K. Katō, Recent development of complex scaling method for many-body resonances and continua in light nuclei, *Prog. Part. Nucl. Phys.* **79**, 1 (2014), [arXiv:1410.4356 \[nucl-th\]](#).
- [73] Y. S. Kalashnikova, Coupled-channel model for charmonium levels and an option for  $X(3872)$ , *Phys. Rev. D* **72**, 034010 (2005), [arXiv:hep-ph/0506270](#).
- [74] S. Coito, G. Rupp, and E. van Beveren,  $X(3872)$  is not a true molecule, *Eur. Phys. J. C* **73**, 2351 (2013), [arXiv:1212.0648 \[hep-ph\]](#).
- [75] E. Cincioglu, J. Nieves, A. Ozpineci, and A. U. Yilmazer, Quarkonium Contribution to Meson Molecules, *Eur. Phys. J. C* **76**, 576 (2016), [arXiv:1606.03239 \[hep-ph\]](#).
- [76] Z.-Y. Zhou and Z. Xiao, Understanding  $X(3862)$ ,  $X(3872)$ , and  $X(3930)$  in a Friedrichs-model-like scheme, *Phys. Rev. D* **96**, 054031 (2017), [Erratum: *Phys.Rev.D* 96, 099905 (2017)], [arXiv:1704.04438 \[hep-ph\]](#).
- [77] F. Giacosa, M. Piotrowska, and S. Coito,  $X(3872)$  as virtual companion pole of the charm-anticharm state  $\chi_{c1}(2P)$ , *Int. J. Mod. Phys. A* **34**, 1950173 (2019), [arXiv:1903.06926 \[hep-ph\]](#).
- [78] G.-J. Wang, Z. Yang, J.-J. Wu, M. Oka, and S.-L. Zhu, New insight into the exotic states strongly coupled with the  $D\bar{D}^*$  from the  $T_{cc}^+$ , (2023), [arXiv:2306.12406 \[hep-ph\]](#).
- [79] H. Li, C. Shi, Y. Chen, M. Gong, J. Liang, Z. Liu, and W. Sun,  $X(3872)$  Relevant  $D\bar{D}^*$  Scattering in  $N_f = 2$  Lattice QCD, (2024), [arXiv:2402.14541 \[hep-lat\]](#).
- [80] W. Kwong, P. B. Mackenzie, R. Rosenfeld, and J. L. Rosner, Quarkonium Annihilation Rates, *Phys. Rev. D* **37**, 3210 (1988).
- [81] W. Kwong and J. L. Rosner,  $D$  Wave Quarkonium Levels of the  $\Upsilon$  Family, *Phys. Rev. D* **38**, 279 (1988).
- [82] V. A. Novikov, L. B. Okun, M. A. Shifman, A. I. Vainshtein, M. B. Voloshin, and V. I. Zakharov, Charmonium and Gluons: Basic Experimental Facts and Theoretical Introduction, *Phys. Rept.* **41**, 1 (1978).
- [83] L. Micu, Decay rates of meson resonances in a quark model, *Nucl. Phys. B* **10**, 521 (1969).
- [84] A. Le Yaouanc, L. Oliver, O. Pene, and J. C. Raynal, Naive quark pair creation model of strong interaction vertices, *Phys. Rev. D* **8**, 2223 (1973).
- [85] V. Bhardwaj *et al.* (Belle), Observation of  $X(3872) \rightarrow J/\psi\gamma$  and search for  $X(3872) \rightarrow \psi'\gamma$  in B decays, *Phys. Rev. Lett.* **107**, 091803 (2011), [arXiv:1105.0177 \[hep-ex\]](#).
- [86] R. Aaij *et al.* (LHCb), Evidence for the decay  $X(3872) \rightarrow \psi(2S)\gamma$ , *Nucl. Phys. B* **886**, 665 (2014), [arXiv:1404.0275 \[hep-ex\]](#).